Electromagnetic Interaction of On-Chip Antennas and CMOS Metal Layers for Wireless IC Interconnects

Ankit More
Drexel University
Department of Electrical and Computer Engineering
Philadelphia, PA 19104, USA
am434@drexel.edu

Baris Taskin
Drexel University
Department of Electrical and Computer Engineering
Philadelphia, PA 19104, USA
taskin@coe.drexel.edu

ABSTRACT

The electromagnetic interaction of on-chip antennas and metal interconnects modeled in a 250 nm complementary metal-oxide semiconductor (CMOS) technology is investigated. A finite element method (FEM) based 3-D full-wave solver is used to perform the electromagnetic field analysis. It is shown that there can be significant signal coupling between the on-chip transmitting antenna and the metal interconnects on a die (-12.09 dB for a 1.6 mm long, 2 μm wide interconnect at a distance of 1 μm from the antenna). Design considerations for metal interconnects in the presence of on-chip antennas are presented in order to limit the undesirable electromagnetic coupling.

Categories and Subject Descriptors

B.4.3 [**Hardware**]: Input/Output and Data Communications—*Interconnections*

General Terms

Design

Keywords

VLSI, interconnects, on-chip antennas, electromagnetic

1. INTRODUCTION

Technology scaling has caused the global interconnects to become one of the major bottlenecks to improvements in IC design, as the interconnect delay is becoming higher than the gate delay [1]. In addition, the system complexity and the die size of a typical integrated circuit have increased significantly. Hence, global interconnect networks, such as the clock distribution network, suffer from skew, jitter, power dissipation and area consumption [2]. Changes to materials of the chip such as low κ dielectrics and high conductivity metals have been introduced to mitigate the effect of the interconnect delay but these changes can increase the scaling of the global interconnect system only by a few technology generations [1]. These considerations have necessitated the need for an alternative global interconnect system to address the growing concerns of timing, power and area overheads. One possible alternative is to use wireless interconnects operating in the radio-frequency (RF) range [3]. The study in [3] demonstrates the feasibility of establishing an intra-chip wireless communication channel for the global delivery of the clock signal. The signal coupling for the wireless communication channel between the transmitting and receiving antenna is shown to be due to wave propagation—not due to conduction through the substrate—demonstrating the true wireless behaviour of intra-chip communication.

In [4], it is shown that the presence of metal interconnects placed on the same layer as that of the antenna in parallel orientation to the antenna decreases the antenna gain in the lower frequency range and increases it in the mid-band and high frequency ranges. However, [4] does not analyze the effect of the radiation from the antennas on the local metal interconnects. Since there are local interconnects present in the same metal layer as that of the antenna, substantial amount of power can be transmitted to these interconnects from the radiations. Hence, it is critical to analyze the transmission gain between the antenna and the local interconnects. Since the interconnects are essentially micro-strip elements, the signal coupling depends heavily on the dimensions of the interconnect.

The novelty of this paper is in characterizing the effect of the radiations on the metal interconnects under varying sizes and topology. In particular, the following scenarios are studied as the contributions of this paper:

1. Interconnects at different metal layers (M1, M2 and M3),
2. Varying widths of the interconnect,
3. Varying lengths of the interconnect,
4. Varying distance of the interconnects from the transmitting antenna.

The effect of the radiation on the local metal interconnects is important as it can greatly influence the overall behaviour of a system using wireless interconnects for intra-chip communication. In particular, the effect of the radiation on the metal interconnects can interfere with the integrity of the signals on the metal interconnect. The criticality of antenna radiation effects on interconnects significantly increases for deep sub-micron technologies as V_{DD} and noise margins for these technologies are much smaller.

Permission to make digital or hard copies of all or part of this work for personal or classroom use is granted without fee provided that copies are not made or distributed for profit or commercial advantage and that copies bear this notice and the full citation on the first page. To copy otherwise, to republish, to post on servers or to redistribute to lists, requires prior specific permission and/or a fee.
GLSVLSI 2010 Providence, Rhode Island USA
Copyright 200X ACM X-XXXXX-XX-X/XX/XX ...$10.00.

2. WIRELESS INTERCONNECT ANALYSIS

The electromagnetic radiation effects of the wireless interconnect system on a die are investigated using an FEM-based full-wave simulation analysis. In particular, the wireless interconnect system is analyzed for the coupling of the transmitting and receiving antennas as well as the (undesirable) coupling between the transmitting antenna and the wire interconnects. The simulation of the wireless interconnect system is performed in Ansoft HFSS (High Frequency Structure Simulator), a 3-D FEM based simulator [5]. The design parameters for the die are selected according to typical 250 nm CMOS technology rules. The 250 nm CMOS semiconductor technology environment is modeled with the parameters presented in Table 1 [6]. The simulation model is shown in Figure 1. The die size is 6 x 4 mm^2 where the antennas are separated at a distance of 5 mm from each other. In the 3-metal layer 250 nm process, the antennas are placed in the third metal layer. In Figure 1, the placement of the interconnect is shown at a distance d from the antenna. The location and the dimensions of the interconnect are varied in order to study the various cases enumerated in Section 1.

Meander dipole antennas are used in the simulation model as these antennas are more compatible with conventional CMOS technologies in having 90° bend angles. The antennas are designed to operate at 17 GHz with a total arm length (including the length of the meander segments) of 2.4 mm according to the parameters presented in [7]. The wavelength of the radiated electromagnetic waves is 6.85 mm based on an effective dielectric constant of 6.61 [8].

The following quantitative variations in geometry and placement of the metal interconnects are studied:

1. Impact on interconnects in different metal layers (3 metal layer process),
2. Impact of varying width of interconnects from 2 μm to 10 μm (all three metal layers),
3. Impact of varying length of interconnects from 100 μm to 3200 μm (M3 layer),
4. Impact of varying distance of interconnects from the transmitting antenna from 1 μm to 4.5 mm (M3 layer).

In items 3 and 4 above, a 2 μm wide, M3 interconnect is used since it is the worst case observed in items 1 and 2.

The metal interconnects are placed parallel to the antenna. This is such as the gain for the dipole antenna is highest in the direction perpendicular to the antenna and at the center of the antenna structure. As the antenna gain is highest at this simulation setup, the worst case interference

Table 1: Material characteristics of different silicon regions on a die.

Material	Conductivity (S/m)	Relative Permittivity
Silicon Dioxide	0	3.7
20 Ω-cm Substrate (lightly doped)	5	11.9
P-type Silicon	800	11.9
N-type Silicon	2300	11.9
P^+/N^+ (active regions)	62500	11.9

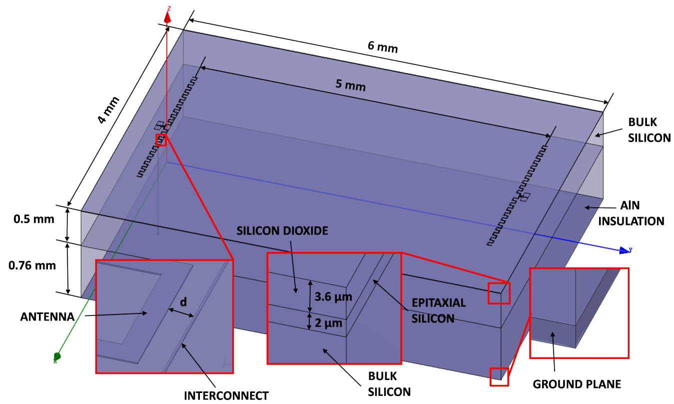

Figure 1: Simulated structure for a wireless interconnect system. Design dimensions are according to a typical 250 nm design technology.

effects on the interconnects are analyzed. The simulations are performed in the frequency range from 10 GHz to 30 GHz as the target operating frequency is 17 GHz.

3. SIMULATION RESULTS

In experimentation, two primary sets of data are collected:

1. The scattering parameter (s-parameter) matrix between the antenna pair, **S**.
2. The transmission s-parameter between the transmitting antenna and the metal interconnects, S_{i1}.

The s-parameter matrix between the antenna pair is used to characterize the operation of the intra-chip wireless communication system. The s-parameter S_{11} (also defined as the radiation loss) characterizes the radiation frequency of the transmitting antenna and the parameter S_{21} characterizes the signal coupling between the radiating and the transmitting antennas. The return loss of the transmitting antenna depicts the frequencies at which the antenna will radiate energy efficiently. It is desired that the return loss be high for the desired bandwidth of frequencies to be transmitted and low for all other frequencies. The transmission gain between the antennas is the figure of merit used to characterize the strength of the signal coupling between the transmitting and receiving antennas. The transmission gain, G_a of the antenna pair is computed using:

$$G_a = \frac{|S_{21}|^2}{(1-|S_{11}|^2)(1-|S_{22}|^2)} = G_t G_r \left(\frac{\lambda}{4\pi R}\right)^2 e^{-2\alpha R} \quad (1)$$

where S_{21} is the forward transmission, S_{11} is the reflection of the electric field at the transmitting antenna and S_{22} is the reflection of the electric field at the receiving antenna. G_t and G_r are the gains of the transmitting an receiving antennas, respectively, λ is the wavelength, α is the attenuation constant and R is the separation. All three parameters S_{11}, S_{21}, and S_{22} are obtained from the s-parameter matrix **S**. The simulation results for the various cases outlined in Section 2 are presented in the following subsections.

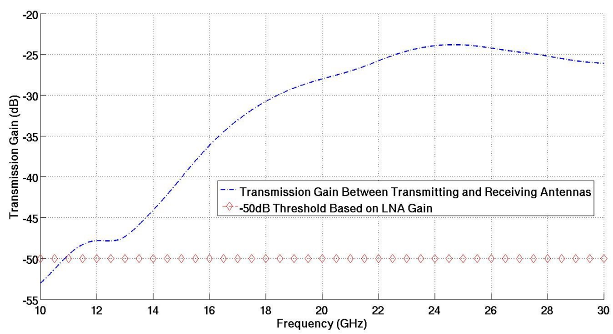

Figure 2: Transmission gain between the transmitting and receiving antennas.

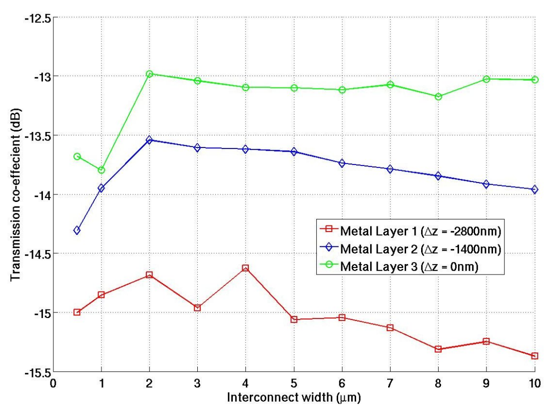

Figure 3: Variation of signal coupling between the interconnect and the transmitting antenna for varying interconnect widths.

3.1 Electromagnetic Coupling Between Transmitting and Receiving Antennas

The computed transmission gain G_a between the transmitting and receiving antennas is shown in Figure 2. For an effective communication, it is required that the gain of the antenna be higher than -50 dB—which is the gain that can be provided using a low noise amplifier (LNA) at the receiving end [9]. At the operating frequency of 17 GHz, a transmission gain of -33.09 dB is observed, proving effective communication.

3.2 Electromagnetic Coupling Between Antenna and Interconnects

The simulation results for the coupling between the metal interconnects and the transmitting antenna show substantial variations under different geometrical sizes and placement. It is desired that the signal coupling between the transmitting antenna and the metal interconnect be low to avoid any signal integrity issues on these interconnects.

3.2.1 Variation with Width and Metal Layer

The transmission s-parameter between the metal interconnect and the transmitting antenna, shown in Figure 3, is used to characterize the signal coupling between the two (2) structures. The transmitting antenna is placed on the M3 layer. The signal coupling between the transmitting antenna and the interconnect decreases with increased metal layer separation between the two structures. The percentage change in signal coupling between the interconnect and the transmitting antenna for placement in different metal layers is shown in Table 2. Note from Figure 3 that the coupling is highest at an interconnect width of 2 μm for placement in all three metal layers. The irregularities in the decreasing trend past 2 μm interconnect width are due to convergence issues in the numerical analysis methods. However, also note that the variation in the transmission s-parameter is not very large with variation in width (approximately 0.5 dB). Thus, the width of the interconnects does not have a major impact on signal coupling.

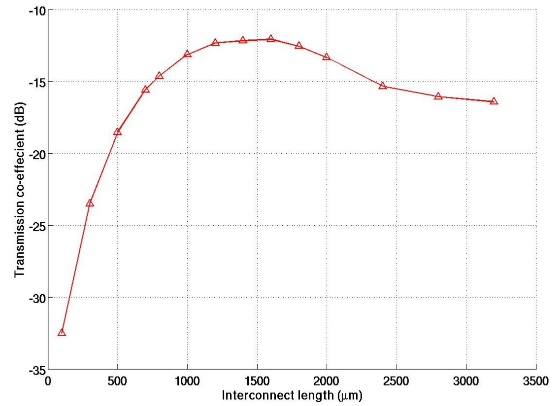

Figure 4: Variation of signal coupling between the interconnect and the transmitting antenna for varying interconnect lengths (interconnect width = 2 μm, distance from antenna = 1 μm).

3.2.2 Variation with Length

The variation of the signal coupling with varying length of the interconnects is significant. The s-parameter between the antenna and the interconnect for varying lengths of a 2 μm wide interconnect placed at a distance of 1 μm is shown in Figure 4. It is observed that the signal coupling is low for small lengths of the interconnects and peaks for lengths at about a quarter of the wavelength ($=6.9/4 \simeq 1.7$ mm) of operation. At quarter wavelength ($\simeq$1.7 mm), the interconnect is behaving as a quarter wave printed monopole antenna [8]. Due to the principle of reciprocity [8], the interconnect also *receives* the maximum amount of energy at this length. The signal coupling is alarmingly high for interconnects longer than 500 μm, however, note that such long lengths of interconnects are generally avoided in integrated circuits. Long interconnects are typically buffered with repeaters, so the coupling impact is low. Note that, depending on the frequency of operation, the wavelength of the electromagnetic waves changes. Therefore, the length of the interconnect—quarter of the wavelength of electromagnetic waves—at which the signal coupling peaks would also change.

3.2.3 Variation with Distance from Antenna

The effect of varying the distance of a 2 μm wide, 1 mm long M3 interconnect from the transmitting antenna is shown in Figure 5. The results for this case are explained using (1). Even though the interconnect is not an antenna, the strength of the electromagnetic waves reduces with distance from the antenna. Thus, the coupling between the antenna and the interconnect also decreases with an increasing distance.

Table 2: Percentage change in the transmission s-parameter between the transmitting antenna and the metal interconnect for different metal layer placements (interconnect width = 2 μm, length = 1 mm).

Metal Layer	Vertical Distance from the Antenna Layer (M3) (nm)	Transmission S-parameter (dB)	% Change in the Transmission S-parameter
M3	0	−12.98	–
M2	−1400	−13.54	4.31%
M1	−2800	−14.69	13.17%

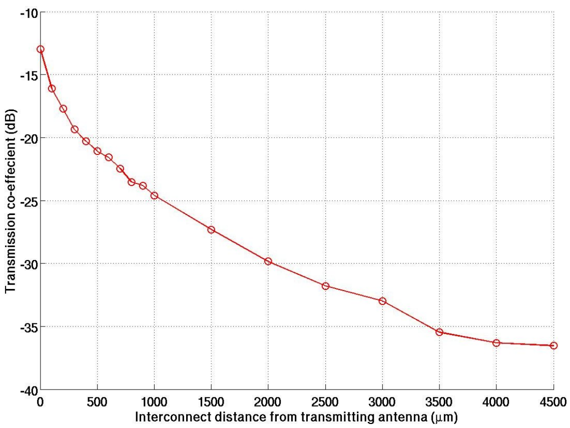

Figure 5: Variation of signal coupling between the interconnect and the transmitting antenna for varying distance of the interconnect from the transmitting antenna (interconnect width = 2 μm, length = 1 mm).

4. SUMMARY OF RESULTS

The presented work shows that there can be substantial coupling between the transmitting antenna and the metal interconnects on the same die. The coupling:

1. Decreases with placement of the interconnect in different metal layers. Lower coupling for higher separation of metal layers is reported (Figure 3 and Table 2),
2. Remains approximately constant with varying width of the interconnect. Peaks at interconnect width of 2 μm but variations are very low (approximately 0.5 dB) (Figure 3),
3. Is very low at small interconnect lengths. Peaks at interconnect length of approximately quarter of the wavelength of the electromagnetic waves (Figure 4),
4. Monotonously decreases with an increasing distance from the transmitting antenna (Figure 5).

Based on these parameters, various design choices can be made with regards to the placement of local metal interconnects to minimize the coupling between the transmitting antenna and the local metal interconnect.

5. CONCLUSION

The effect of the electromagnetic radiations from antennas integrated on chips with the metal interconnects is demonstrated. The antenna characteristics of on-chip integrated antennas, for intra-chip interconnection under typical 250 nm standard CMOS technology parameters is investigated. The simulation model of the die for the 3-D FEM based full-wave analysis adheres to the typical manufacturing process requirements. It is shown in this paper that the electromagnetic radiations from the antennas can cause significant coupling between the metal interconnects and the transmitting antenna depending on the geometry and placement of the interconnects. The coupling between the interconnects and the transmitting antenna is undesirable and can cause signal integrity problems.

These simulation results show that it is possible for a radio frequency (RF) wireless interconnects system to have good electromagnetic compatibility and low electromagnetic interference with the metal interconnects on a die. The design considerations for the interconnect geometry and placement with respect to the antenna specifications must be integrated in to the physical design automation processes.

6. REFERENCES

[1] *ITRS International Technology Roadmap for Semiconductors*, 2006.

[2] V. Mehrotra and D. Boning, "Technology scaling impact of variation on clock skew and interconnect to silicon," in *Proceedings of the IEEE International Interconnect Technology Conference (IITC)*, June 2001, pp. 122–124.

[3] B. A. Floyd, C. M. Hung, and K. K. O, "Intra-chip wireless interconnect for clock distribution implemented with integrated antennas, receivers and transmitters," *IEEE Journal of Solid-State Circuits*, vol. 37, pp. 543–551, May 2002.

[4] M. Bialkowski and A. Abbosh, "Investigations into intra chip wireless interconnection for ultra large scale integration technology," in *Proceedings of the IEEE Antennas and Propagation Society International Symposium (APSURSI)*, June, pp. 1–4.

[5] *High Frequency Structure Simulator: User's Guide*, 10th ed., Ansoft Corporation, June 2005.

[6] S. Bronckers, K. Scheir, G. V. Plas, G. Vandersteen, and Y. Rolain, "A methodology to predict the impact of substrate noise in analog/RF systems," *IEEE Transactions on Computer-Aided Design of Integrated Circuit and Systems*, vol. 28, pp. 1613–1626, November 2009.

[7] H. Nakano, H. Tagami, A. Yoshizawa, and J. Yamauchi, "Sortening ratios of modified dipole antennas," *IEEE Transactions on Antennas and Propagation*, vol. 32, pp. 385–386, April 1984.

[8] D. M. Pozar, *Microwave Engineering*, 3rd ed. Wiley, 2005.

[9] A. B. M. H. Rashid, N. Sultana, M. R. Khan, and T. Kikkawa, "Efficient design of integrated antennas on si for on-chip wireless interconnects in multi-layer metal process," *Japanese Journal of Applied Physics*, vol. 44, pp. 2756–2760, April 2005.